Simulation study on heat transfer characteristics of spray cooled serpentine coil

Zhaoyi Chen, Zhi Liu, Kaiyong Hu[a,*]

Tianjin Key Lab of Refrigeration Technology, Tianjin University of Commerce, No.409 Guangrong Road, Tianjin, 300134, China

[a]chenzhaoe@yeah.net

*Corresponding author

Keywords: Spray cooling; Number of nozzles; CFD

Abstract: Improving a heat exchanger's heat transfer capability is essential for energy conservation. An important factor in promoting heat transfer between hot and cold fluids is the heat exchanger's coil. As a result, increasing the coil's heat transfer capacity is essential to raising the heat exchanger's overall performance. Spray cooling technology is renowned for its superior capacity to transfer heat. This study examines how spray cooling technology can be applied to a serpentine coil and examines how different spray cooling settings affect the coil's heat transfer properties. While faster droplet evaporation rates lead to higher relative humidity at the air outlet—albeit with a thicker liquid film—increasing the spray density can increase the heat flux on the coil's surface. Furthermore, a greater number of nozzles distributes droplets more widely, improving droplet evaporation rates and heat flux on the coil's surface. As a result, the liquid film thickness decreases and relative humidity at the air exit rises.

1. Introduction

Enhancing the heat transfer capacity of heat exchangers is a prominent area of research, with a particular focus on enhancing the heat transfer efficiency of cooling towers and evaporative condensers as evidenced by previous studies [1,2]. The optimization of heat exchanger performance is crucial for energy conservation, underscoring the need for further research in this field. Within heat exchangers, particularly in closed cooling towers and evaporative condensers, the coil serves as a vital conduit for heat exchange between hot and cold fluids. Therefore, enhancing the heat transfer capacity of the coil is essential for improving the overall heat transfer efficiency of the heat exchanger.

The enhancement of heat transfer in coils can be achieved through active technology or passive technology [3]. Passive technology is generally more cost-effective, but once the material and structure of the heat exchanger are determined, active technology research becomes crucial due to the high cost of metal coil pipes. Spray cooling technology, known for its high heat flux and minimal cooling medium requirement [4], can effectively enhance the heat transfer capacity of coils. The atomization parameters in spray cooling technology, such as spray density and nozzle number, are key factors that influence the heat transfer capacity [5,6]. Therefore, understanding and optimizing these parameters are essential for improving heat transfer efficiency in spray cooling technology.

The application of spray cooling technology in the coil is anticipated to enhance its heat transfer capacity. However, previous studies have only simplified the coil as a horizontal straight tube [5], with few simulations of serpentine tubes in the reduction coil. Therefore, this paper has developed a physical model of the serpentine coil and utilized spray cooling technology to investigate the heat transfer characteristics of the serpentine coil by analyzing spray density and the number of nozzles. It is hoped that this study can serve as a reference for enhancing the heat transfer efficiency of coils.

  DOI: 10.25236/icmmct.2024.019

2. Methods

2.1. Geometry

Fig. 1 illustrates the schematic diagram of the simulation model. The model has overall dimensions of 600mm×110mm×75mm and consists of a coil made up of three serpentine tubes. Each tube has a diameter of 10mm and is spaced longitudinally at 25mm intervals. The top and bottom rows of serpentine tubes have a length of 85mm, while the middle row is 60mm long, with a 25mm distance between the tubes. To enhance heat transfer efficiency, air is introduced to mimic the effect of an axial fan. The bottom of the physical model serves as an air velocity inlet, while the top acts as an air pressure outlet. Additionally, symmetrical boundaries are set on the walls flanking the coil. The nozzle is positioned below the coil, with gravity acceleration directed as depicted in the figure.

In this study, the finite element volume method is employed to compute the control equation. The model is initially discretized through grid division, followed by specific calculations with boundary conditions set for air, pipe wall, and spray. The coupling solution of the velocity field and pressure field is achieved using the standard SIMPLE algorithm based on a pressure solver. Convergence is determined by ensuring that the relative change rate of heat flux density on the outer wall of the monitoring tube is below 10^{-6}.

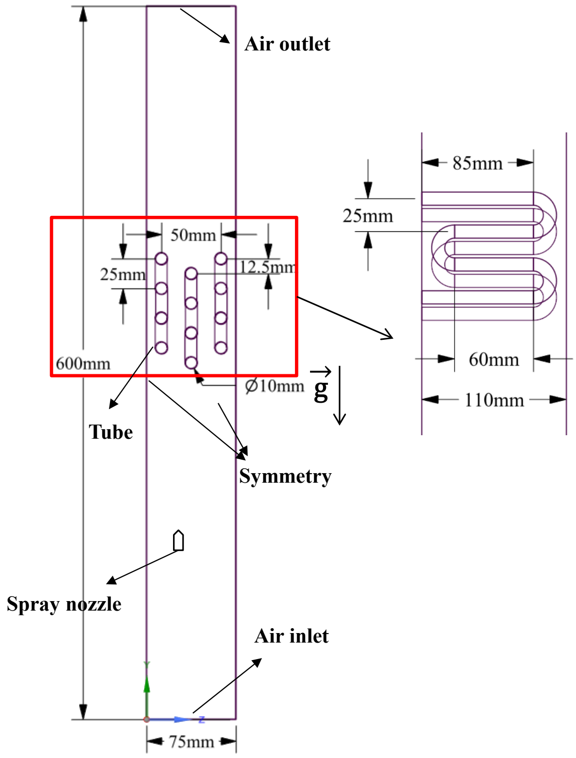

Figure 1: Physical model of spray cooling coils.

2.2. Physical models and governing equations

Computational fluid dynamics (CFD) has been extensively utilized for simulating spray cooling. In these simulations, air is typically considered as a continuous phase while spray droplets are treated as a discrete phase. The fluid flow is governed by three conservation equations, and the evaporation of individual droplets influences the continuous phase, necessitating the incorporation of a component transport model. To enhance computational efficiency, several assumptions are made: (1) droplets are assumed to be spherical, (2) the coil wall is considered a non-slip wall with no convection, heat transfer, or radiation in the tube, and the wall is maintained at a constant temperature of 333.15K, (3) there is no heat transfer between the outer wall of the model and the surrounding air, and (4) air is assumed to be an incompressible fluid with constant physical properties.

2.2.1. Continuous phase model

(1) Conservation of mass equation

$$\frac{\partial \rho}{\partial t}+\frac{\partial}{\partial x_i}(\rho u_i)=S_m \tag{1}$$

Where ρ is the density; t is the system time; u_i is the continuous phase velocity field; S_m is the mass source term.

(2) Conservation of momentum equation

$$\frac{\partial}{\partial t}(\rho u_i)+\frac{\partial}{\partial x_i}(\rho u_i u_j)=-\frac{\partial P}{\partial x_i}+\frac{\partial}{\partial x_i}\left(\mu\frac{\partial u_i}{\partial x_j}\right)+S_{u_i} \tag{2}$$

Where μ is the continuous phase viscosity; P is the pressure; S_{u_i} is the momentum source term.

(3)Conservation of energy equation

$$\frac{\partial}{\partial t}(\rho u_i E)+\frac{\partial}{\partial x_i}\left(u_i(\rho E+P)\right)=\frac{\partial}{\partial x_i}\left(k_e\nabla T-\sum_j J_j\int_{T_{ref}}^{T}C_{P,j}dT+(\tau_e\cdot u_i)\right)+S_h \tag{3}$$

Where E is the total energy; k_e is the effective thermal conductivity; J_j is the diffusion flux from the species j; $C_{P,j}$ is the heat capacity of the species j in the continuous phase; S_h is the energy source term.

(4) Species transport

$$\frac{\partial}{\partial t}(\rho u_i E)+\frac{\partial}{\partial x_i}\left(u_i(\rho E+P)\right)=\frac{\partial}{\partial x_i}\left(k_e\nabla T-\sum_j J_j\int_{T_{ref}}^{T}C_{P,j}dT+(\tau_e\cdot u_i)\right)+S_h \tag{4}$$

Where Y_i is the local mass fraction of the different components; R_i is the net rate of generation of species by chemical reactions; S_i is the source term resulting from the phase transition of the discrete phase, and $\vec{J_i}$ is the diffusion flux from the species, which can be next two cases according to the different flows:

For laminar flow:

$$\vec{J_i}=-\rho D_{i,m}\nabla Y_i-D_{i,h}\frac{\nabla T}{T} \tag{5}$$

Where $D_{i,m}$ is the mass diffusion coefficient of the mixed component; $D_{i,h}$ is the thermal diffusion coefficient of the mixed component.

For turbulent flow:

$$\vec{J_i}=-\left(\rho D_{i,m}+\frac{\mu_t}{Sc_t}\right)\nabla Y_i-D_{i,h}\frac{\nabla T}{T} \tag{6}$$

Where μ_t is the turbulent viscosity; Sc_t is turbulent Schmidt number.

2.2.2. Dispersed phase model

The description of the discrete term can be described by Newton's second law to describe the gravity, air resistance and buoyancy of the droplets in the discrete phase.

$$m_p\frac{du_p}{dt}=m_p\vec{g}-m_p\frac{u_p-u_i}{\tau_p}-m_p\vec{g}\frac{\rho}{\rho_p} \tag{7}$$

Where m_p is the mass of the droplet; u_p is the velocity of the droplet; ρ_p is the density of the droplet. the right side of equation (7) is the gravitational force on the droplet, and the resistance and buoyancy by the air, respectively; τ_p is the relaxation time of the droplet.

2.2.3. Realizable k-epsilon model

Realizable k-epsilon model can be applied to free flow, jet flow, boundary layer flow and so on. Because the droplets are sprayed in the air and hit the hot surface for heat transfer, the degree of turbulence is high, and the Realizable k-epsilon model has been applied more in spray simulation [7,8], so this paper also selects the Realizable k-epsilon model to describe the turbulence.

2.2.4. Heat and mass transfer to the droplet

There exists not only heat transfer imagery but also mass transfer phenomenon between the liquid droplets in the discrete phase and the air in the continuous phase, and the radiative heat transfer is neglected in this simulation, so the heat balance equation of the droplet particles can be written as the sum of the sensible heat change and the latent heat change [8]:

$$m_p C_p \frac{dT_p}{dt} = h_c A_p \left(T_\infty - T_p\right) - \frac{dm_p}{dt} h_{fg} \tag{8}$$

Where C_p is the specific heat capacity; A_p is the droplet-air contact area; h_c is the convective heat transfer coefficient; h_{fg} is the latent heat; $\frac{dm_p}{dt}$ is the evaporation rate. At the same time, the droplet will be attached to the outer wall of the coil, and the Lagrangian liquid film model can be applied to analyze the droplet's motion on the wall. In this model, the discrete term boundary layer of the wall is designated as 'wall-film'.

2.3. Mesh

The focus of this study is the heat transfer characteristic of the outer wall of the coil. The mesh on the outer wall of the serpentine coil is refined through expanding the boundary layer. To ensure minimal influence of grid quality on simulation results, the model is verified for grid independence. The results are presented in figure 2. As shown in the figure, the average heat flux density on the pipe wall changes gradually with an increase in the number of grids. When the number of grids reaches 885,987, the difference in average heat flux density between the coil surface and 984,593 grids is 0.34%. It can be concluded that when the number of grids reaches 885,987, the change in heat flux density with the number of grids becomes negligible. Therefore, for computational efficiency, subsequent simulations will be conducted using a grid with 885,987 cells.

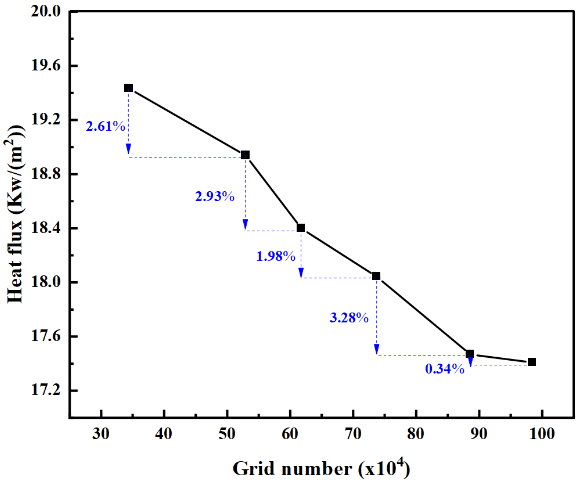

Figure 2: Results of mesh independence test.

3. Results and discussion

3.1. Effect of spray density

The impact of spray density on the surface heat flux and droplet evaporation rate of serpentine coil bundles is illustrated in Figure 3. The figure demonstrates that both the heat flux and evaporation rate of the coils rise as the spray density increases. An increase in spray density leads to more droplets engaging in heat transfer with the coil, resulting in the formation of a larger liquid film on the coil surface. This film reduces heat transfer between the coil and the air, while enhancing heat transfer between the coil and the liquid film, consequently elevating the heat flux on the coil surface. Moreover, the higher density of droplets increases the heat transfer area between the droplet and the coil, thereby boosting the droplet's evaporation rate.

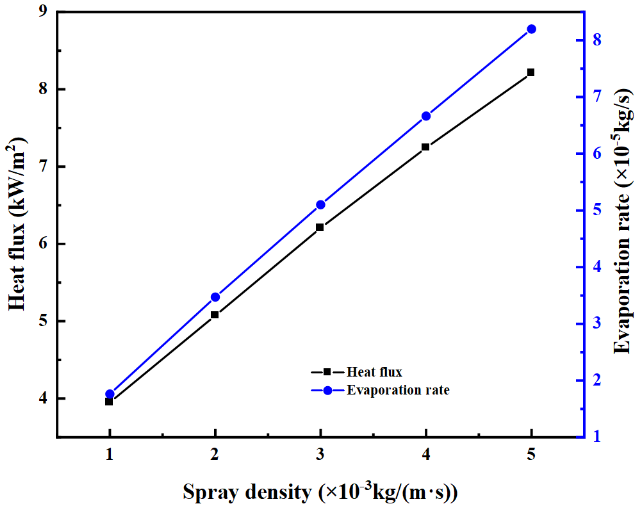

Figure 3: Effect of spray density on heat flux and droplet evaporation rate.

The impact of spray density on the thickness of the liquid film on the coil surface and the relative humidity of the air outlet is illustrated in Figure 4. The data demonstrates that both the thickness of the liquid film on the coil surface and the relative humidity of the air outlet rise as the spray density increases. This is due to the augmented number of droplets that come into contact with the coil surface with increasing spray density. Consequently, the drying area of the coil surface decreases, leading to a wider distribution range of the liquid film and ultimately an increase in its thickness. Simultaneously, the higher number of droplets results in an increased rate of evaporation, leading to elevated air temperature and moisture content, thereby causing an increase in the relative humidity of the air outlet.

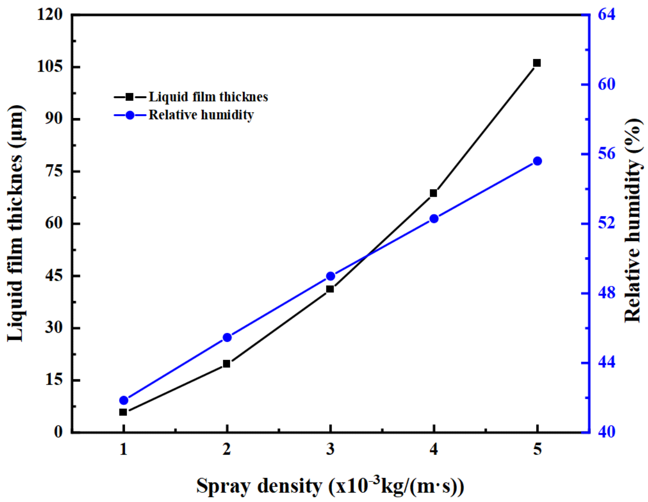

Figure 4: Effect of spray density on liquid film thickness and relative humidity at air outlet.

3.2. Effect of the number of nozzles

The impact of varying the number of nozzles on the heat flux on the coil surface and the evaporation rate of droplets is depicted in Figure 5. The figure illustrates that an increase in the number of nozzles results in a higher heat flux on the coil surface and a corresponding rise in the evaporation rate of droplets. When the mass flow rate of the spray remains constant, enhancing the number of nozzles can enhance the distribution of droplets on the coil, leading to an increase in the heat flux on the coil surface. This increased distribution of droplets also enlarges the contact area between droplets and the pipe wall, consequently elevating the evaporation rate. However, as the number of nozzles increases, the proximity between adjacent nozzles decreases within a specific volume, causing an overlapping area in the spray zone. This overlap leads to a thicker liquid film and reduces the perturbation of droplets on the liquid film.

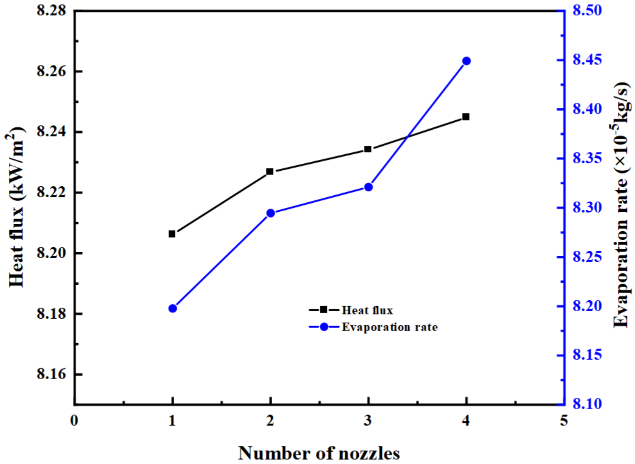

Figure 5: Effect of nozzle number on heat flux and droplet evaporation rate.

The impact of varying the number of nozzles on the thickness of the liquid film on the coil surface and the relative humidity of the air outlet is depicted in figure 6. The figure illustrates a decrease in the liquid film thickness on the coil surface with an increase in the number of nozzles, while the relative humidity at the air outlet shows a gradual increase. As discussed earlier, the wider spray distribution resulting from an increased number of nozzles, under a constant mass flow rate, enhances the contact area between the droplet and the coil. This leads to an increase in the evaporation rate and subsequently raises the relative humidity at the air outlet. Although increasing the number of nozzles reduces the mass flow rate per nozzle while maintaining a constant overall mass flow rate, it results in a larger distribution range. Consequently, the thickness of the liquid film on the coil surface decreases, but the distribution area expands.

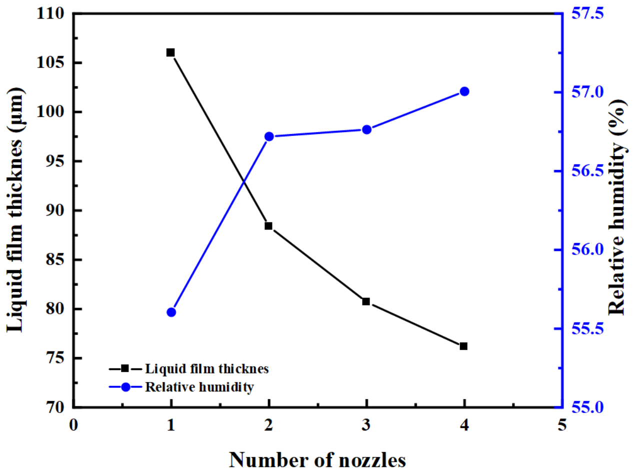

Figure 6: Effect of nozzle number on liquid film thickness and air outlet relative humidity.

4. Conclusions

This paper aims to investigate the impact of spray cooling technology on the heat transfer performance of serpentine coils. The study utilizes numerical simulation to analyze the cooling effect of spray on the serpentine coil, and examines the influence on the coil's heat transfer capacity by varying spray parameters such as spray density and number of nozzles. The main findings of the study are as follows:

(1) As spray density increases, heat transfer shifts from coil-to-air to coil-to-droplet, enhancing coil heat transfer and increasing droplet evaporation rate, resulting in higher relative humidity at the air outlet. Higher spray density also promotes the formation of a liquid film.

(2) Increasing the number of nozzles improves liquid droplet distribution and liquid film coverage, but reduces average liquid film thickness. Greater coverage of the liquid film increases the surface area of the coil covered by a thin film, enhancing coil heat transfer, increasing droplet evaporation rate, and raising relative humidity at the air outlet.

References

[1] Zhao, R., Bu, S., Zhao, X., Zhang, L., Xu, W., Yu, Z., Bao, B. (2021). Study on thermal performance of new finned heat exchange tube bundles in cooling tower. International Journal of Thermal Sciences, 168, 107064.

[2] Fiorentino, M., Starace, G. (2018). The design of countercurrent evaporative condensers with the hybrid method. Applied Thermal Engineering, 130, 889-898.

[3] Ghogare, R. M., Gore, V. G., Shaikh, A. S. (2018). A review of passive technique used for heat transfer enhancement in heat exchanger. International Research Journal of Engineering and Technology, 5(2), 571-576.

[4] Huang, Y., Wang, M., Xu, L., Deng, J. (2021). Experimental study on a spray and falling-film cooling system. Case Studies in Thermal Engineering, 26, 101057.

[5] Zeng, Z., Li, Y., Shang, T., Zhan, H. (2023). Effects of the atomisation spray on heating transfer in evaporative condensers: A numerical study. Thermal Science and Engineering Progress, 42, 101923.

[6] Hou, Y., Tao, Y., Huai, X., Zou, Y., Sun, D. (2018). Numerical simulation of multi-nozzle spray cooling heat transfer. international journal of thermal sciences, 125, 81-88.

[7] Wan, H., Liu, P. J., He, G. Q., Xue, Z. R., Qin, F., & Li, W. Q. (2023). Experimental and numerical studies on the spray cooling of deionized water in non-boiling regime. Case Studies in Thermal Engineering, 44, 102834.

[8] Ansys Fluent Theory Guide, ANSYS Inc., USA, 2013, pp. 724–746. 15317.